JOURNAL OF MATERIALS SCIENCE **36** (2001) 723–729

Ultrasonic study of the elastic and nonlinear acoustic properties of ceramic aluminum nitride

S. P. DODD, G. A. SAUNDERS
Department of Physics, University of Bath, Bath BA2 7AY, UK

M. CANKURTARAN
Department of Physics, Hacettepe University, Beytepe, 06532 Ankara, Turkey

B. JAMES
DERA, LSAB1, Chobham Lane, Chertsey, Surrey KT16 OEE, UK

Pulse-echo-overlap measurements of ultrasonic wave velocity have been used to determine the elastic stiffness moduli and related elastic properties of aluminum nitride (AlN) ceramic samples as functions of temperature in the range 100–295 K and hydrostatic pressure up to 0.2 GPa at room temperature. Aluminum nitride is an elastically stiff but light ceramic: at 295 K, the longitudinal stiffness (C_L), shear stiffness (μ), adiabatic bulk modulus (B^S), Young's modulus (E) and Poisson's ratio (σ) are 373 GPa, 130 GPa, 200 GPa, 320 GPa and 0.234, respectively. The temperature dependences of C_L and B^S show normal behaviour and can be approximated by the conventional model for vibrational anharmonicity. The results of measurements of the effects of hydrostatic pressure on the ultrasonic wave velocity have been used to determine the hydrostatic-pressure derivatives of elastic stiffnesses and the acoustic-mode Grüneisen parameters. The values determined at 295 K for the hydrostatic-pressure derivatives $(\partial C_L/\partial P)_{P=0}$, $(\partial \mu/\partial P)_{P=0}$ and $(\partial B^S/\partial P)_{P=0}$ are 4.7 ± 0.1, 0.22 ± 0.03 and 4.4 ± 0.15, respectively. The adiabatic bulk modulus B^S and its hydrostatic-pressure derivative $(\partial B^S/\partial P)_{P=0}$ are in good agreement with the results of recent high pressure X-ray diffraction measurements and theoretical calculations. The longitudinal (γ_L), shear (γ_S), and mean (γ^{el}) acoustic-mode Grüneisen parameters of AlN are positive: the zone-centre acoustic phonons stiffen under pressure. The shear γ_S (=0.006) is much smaller than the longitudinal γ_L (=1.09) accounting for the low thermal Grüneisen parameter γ^{th} (=0.65) obtained for this ceramic: since the acoustic Debye temperature Θ_D (=980 ± 5 K) is so high, the shear modes play an important role in acoustic phonon population at room temperature. Hence knowledge of the elastic and nonlinear acoustic properties sheds light on the thermal properties of ceramic AlN.

1. Introduction

Aluminum nitride (AlN) is an insulator (or wide-band-gap semiconductor with a direct band gap of 6.2 eV [1]) which is of considerable importance in electronic technology due to its high thermal conductivity, low thermal expansion, high strength, transparency, and piezoelectric properties. At ambient conditions AlN crystallizes in the hexagonal wurtzite structure; it is a tetrahedrally coordinated III-V compound with interionic bonding that can be regarded as partially ionic and partially covalent. Despite the technological importance of AlN, understanding of the elastic and nonlinear acoustic properties of its ceramic form is sparse. Previously the elastic moduli of hot pressed AlN have been measured [2] in a relatively narrow temperature range from room temperature down to 273 K and under uniaxial pressure (at room temperature) by a cw resonance technique. Several theoretical calculations, made using different methods, of the elastic properties of AlN have recently been published (for an overview, see [3]). The present high-pressure ultrasonic study of the elastic and nonlinear acoustic properties of AlN has been largely motivated by these theoretical calculations of the bulk modulus of AlN and its pressure derivative, since some of them predicted considerably different results than those reported in [2]. In the present work ultrasonic wave velocity measurements in hot-pressed AlN ceramic have been extended down to 100 K. To assess the nonlinear acoustic properties of AlN, ultrasonic wave velocities have been measured as a function of hydrostatic pressure up to 0.2 GPa at room temperature. The outcome of this experimental work has been the determination of the technological elastic stiffness moduli and related elastic properties and how they vary with temperature and hydrostatic pressure. The elastic stiffnesses of a material determine the slopes of the acoustic-phonon

dispersion curves in the long-wavelength limit; their hydrostatic-pressure dependences provide information on the shift of the mode energies with compression and hence on the anharmonicity of zone-centre acoustic phonons. The present results provide intriguing physical insight into the elastic and nonlinear acoustic properties and in turn on the thermal properties of ceramic AlN.

2. Experimental procedures

The AlN ceramic was manufactured by Cercom (USA). Scanning electron microscope images of the grain structure were taken on suitably polished and thermally etched samples (Fig. 1). The grains are randomly oriented and have a range of sizes. To obtain a measure of average grain size, a lineal intercept analysis was performed: the intercept length for 1000 grains was measured. Actual grain sizes (d) were calculated using the expression

$$d = 1.56(L/m_f), \tag{1}$$

where L is the measured lineal intercept length and m_f is the magnification factor used in the scanning electron microscope. The factor 1.56 is an effective correction factor derived by Mendelson [4] for random slices through a model system consisting of space filling tetrakaidecahedrally shaped grains (truncated octahedrons) with a log-normal size distribution. The ceramic was considered to be single phase. This assumption is valid considering the very low secondary phase content and low porosity. The grain size distribution is shown in Fig. 2. Average grain size for this AlN ceramic was calculated to be 4.18 ± 2.75 μm. The sample density (3260 ± 10 kg m^{-3}) was measured by Archimedes' method using distilled water as a flotation fluid. The density of the sample is, within the experimental error, equal to the theoretical density (3280 kg m^{-3}) of pure AlN. A sample, which was large enough for precision measurements of ultrasonic wave velocities, was cut and polished with a pair of faces, flat to surface irregularities of about 3 μm and parallel to better than 10^{-3} rad. The sample thickness in the direction of ultrasonic wave propagation was 9.699 ± 0.002 mm.

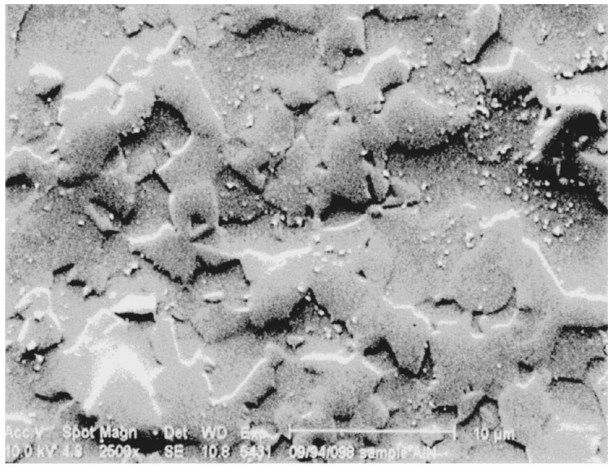

Figure 1 Scanning electron microscope image of the grain structure of AlN ceramic sample.

To generate and detect ultrasonic pulses, X- or Y-cut (for longitudinal and shear waves, respectively) 10-MHz quartz transducers operated in the 30 MHz overtone were bonded to the specimen using Nonaq stopcock grease for low-temperature experiments. Dow resin was used as bonding material for high-pressure experiments. Ultrasonic pulse transit times were measured using a pulse-echo-overlap system [5], capable of resolution of velocity changes to 1 part in 10^5 and particularly well suited to determination of pressure- or temperature-induced changes in velocity. A correction was applied to the ultrasonic wave velocity for multiple reflections at the sample transducer interface [6]. The temperature dependence of ultrasound velocity was measured between 100 and 295 K using a closed-cycle cryostat. At temperatures lower than about 100 K thermal expansion differences between sample, bond and transducer caused the ultrasonic signal to be lost. A number of bonding agents were tried, but none gave satisfactory results below this temperature. The dependence of ultrasonic wave velocity upon hydrostatic pressure was measured at room temperature (295 K). Hydrostatic pressure up to 0.2 GPa was applied in a piston-and-cylinder apparatus using silicone oil as the pressure-transmitting medium. Pressure was measured using a pre-calibrated manganin resistance gauge. Pressure-induced changes in the sample dimensions were accounted for by using the "natural velocity (W)" technique [7].

3. Temperature dependence of the elastic stiffness moduli

The velocities of longitudinal (V_L) and shear (V_S) ultrasonic waves propagated in the AlN ceramic at 295 K are given in Table I. This small-grained polycrystalline ceramic can be treated as an isotropic material, which has two independent elastic stiffness moduli C_L ($=\rho V_L^2$) and μ ($=\rho V_S^2$), because the ultrasonic wavelength is about two orders of magnitude larger than the average grain size. These elastic stiffness moduli, the adiabatic bulk modulus B^S, Young's modulus E, Poisson's ratio σ, and the acoustic Debye temperature Θ_D have been determined at room temperature, using the ultrasonic velocity data and sample density ρ, and compared where possible in Table I with those reported in the literature.

Both the longitudinal and shear ultrasonic wave velocities (and hence the related elastic moduli) determined in this work are in good agreement with those quoted in [8, 9] for commercial AlN ceramic samples (Dow Chemical Co, MI). We note that the experimental method used for elastic property measurements was not mentioned in [8, 9]. Although the density of the AlN ceramic used by Gerlich *et al.* [2] is similar to that of ours, the value of the longitudinal wave velocity measured by them is about 5% smaller than that determined in the present work; this accounts for

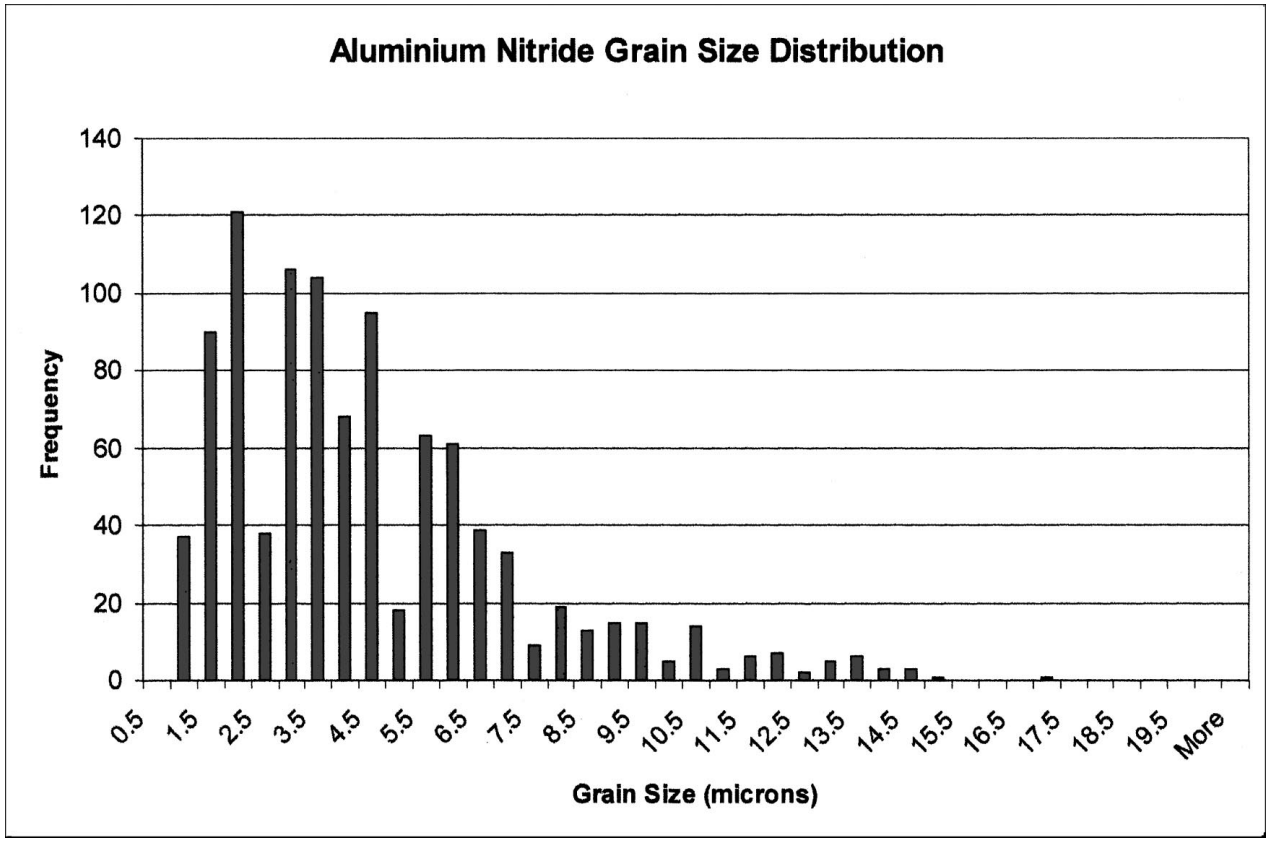

Figure 2 The grain size distribution in the AlN ceramic sample. Average grain size was found to be 4.18 ± 2.75 μm.

TABLE I The ultrasonic wave velocities, adiabatic elastic stiffness moduli and their hydrostatic-pressure derivatives, and the acoustic-mode Grüneisen parameters of ceramic AlN at 295 K, in comparison with data taken from literature

Description	Present work	Ref. [2]	Ref. [8]	Ref. [9]
Density ρ (kg m^{-3})	3260 ± 10	3270	3226	3250
Longitudinal wave velocity V_L (m s^{-1})	10700 ± 10	10127	10720	10700
Shear wave velocity V_S (m s^{-1})	6307 ± 10	6333	6270	6300
Longitudinal stiffness C_L (GPa)	373 ± 2	334.3		
Shear stiffness μ (GPa)	130 ± 1	130.8	127	129
Bulk modulus B^S (GPa)	200 ± 2	159.9	201	203
Young's modulus E (GPa)	320 ± 3	308.3	314	320
Poisson's ratio σ	0.234 ± 0.002	0.179	0.238	0.237
Acoustic Debye temperature Θ_D (K)	980 ± 5			
$(\partial C_L/\partial P)_{P=0}$	4.7 ± 0.1	5.5 ± 0.7		
$(\partial \mu/\partial P)_{P=0}$	0.22 ± 0.03	0.2 ± 2		
$(\partial B^S/\partial P)_{P=0}$	4.4 ± 0.15	5.2 ± 4		
γ_L	1.09 ± 0.02	1.16		
γ_S	0.006 ± 0.01	-0.01		
γ^{el}	0.37 ± 0.02	0.38		
γ^{th}	0.65	0.45		

the differences found between the values of C_L, B^S, E and σ (Table I). Our values for the longitudinal and shear wave velocities in AlN ceramic are in excellent agreement with those ($V_L = 10700$ m s^{-1} and $V_S = 6200$ m s^{-1}) derived from the results of time-of-flight neutron spectroscopy measurements using a polycrystalline AlN sample in combination with theoretical calculations [10]. The acoustic Debye temperature (980 ± 5 K) determined in the present work is in accord with that ($\cong$983 K at room temperature) deduced from lattice specific heat of AlN given in [10] and with that (=950 K at zero K) quoted in [11]. Nipko and Loong [10] calculated the phonon dispersion curves of AlN along major symmetry directions: the steep longitudinal- and shear-acoustic branches, and the high cut-off frequency (i.e., high acoustic Debye temperature) are consistent with the high stiffness and mechanical strength of the material.

The value determined for the adiabatic bulk modulus of AlN ceramic is in good agreement with the results of most of the previous experimental studies and theoretical calculations (Table II). The growth of single crystals of AlN has proved difficult primarily due to the high melting temperature and the decomposition of the material at temperatures approaching the melting point [28, 29]. Only small (at most mm size) single crystals have been grown so far; large enough single crystals of AlN are unavailable for ultrasonic pulse-echo measurements. Only limited data at room temperature are available for the single-crystal elastic constants (C_{IJ}) of AlN. All the five independent elastic constants of single-crystal AlN were derived from surface acoustic wave (SAW) measurements in epitaxial-grown thin films [14], Brillouin light scattering experiments on small platelet-shaped crystals [15] and preferentially oriented, sputtered polycrystalline films [16]. Recently, Deger *et al.* [17] reported the elastic constants of wurtzite structure AlN measured by using SAW on Al_xGaN_{1-x} thin films. The adiabatic bulk modulus B^S determined in this work for high-density AlN ceramic at room temperature is compared in Table II

TABLE II A comparison between the adiabatic bulk modulus B^S and its hydrostatic-pressure derivative $(\partial B^S/\partial P)_{P=0}$ determined for AlN ceramic at room temperature and the results of previous ultrasonic experiments under uniaxial pressure, very-high pressure X-ray diffraction measurements and theoretical calculations. (LCAO: linear combination of atomic orbitals; LDA: local density approximation; OLCAO: orthogonolized linear combination of atomic orbitals; LMTO: linear muffin-tin orbitals)

Bulk modulus (GPa)	Pressure-derivative of bulk modulus	Method	Reference
		Experiment	
200 ± 2	4.4 ± 0.1	Ultrasonic, pulse-echo overlap	Present work
159.9	5.2 ± 4	Ultrasonic, cw resonance	[2]
207.9 ± 6.3	6.3 ± 0.9	X-ray diffraction	[12]
185.0 ± 5.0	5.7 ± 1.0	X-ray diffraction	[13]
201	—	Surface acoustic waves	[14]
210	—	Brillouin scattering	[15]
193, 206	—	Brillouin scattering	[16]
209	—	Surface acoustic waves	[17]
		Theory	
207	3.98	LCAO	[18]
195	3.74	pseudopotential-LDA	[19]
207	5.60	OLCAO-LDA	[20]
237–243	3.77–4.45	Hartree-Fock	[21]
202	3.8	LMTO-FP	[22]
198	4.764	empirical interatomic potentials	[23]
205	—	LMTO-FP	[24]
194	—	pseudopotential-LDA	[25]
207	—	pseudopotential-LDA	[26]
207	—	pseudopotential-LDA	[27]
212	—	first principles-total energy	[3]

with the bulk modulus calculated from single-crystal elastic constants [14–17] using

$$B = \frac{(C_{11} + C_{12})C_{33} - 2C_{13}^2}{C_{11} + C_{12} + 2C_{33} - 4C_{13}}. \qquad (2)$$

Table II also includes the results of very-high pressure X-ray diffraction measurements [12, 30] and theoretical calculations [3, 18–27]. The adiabatic bulk modulus of AlN ceramic determined in this work is in good agreement (within 5%) with the bulk modulus estimated from single-crystal elastic constants, that obtained from very-high pressure X-ray diffraction measurements, and that derived from theoretical calculations (see also [30]). This observation indicates that there is a good bonding between the grains and a lower density of microstructural defects such as microcracks in the AlN ceramic sample used in the present work; hence its elastic properties (Table I) can be considered as representative for polycrystalline AlN.

The temperature dependences of the longitudinal C_L and shear μ elastic stiffnesses, bulk modulus B^S, Young's modulus E and acoustic Debye temperature Θ_D are shown in Fig. 3. They were obtained from the sample density and the velocities of 30 MHz ultrasonic waves propagated in the AlN ceramic sample as it was cycled between room temperature and 100 K. There was no thermal hysteresis in the ultrasonic wave velocities and no irreversible effects, again evidencing the good intergranular bonding. Corrections on elastic moduli for sample length and density changes are expected to be negligible due to the low thermal expansion of AlN [9, 11]. All elastic moduli increase with decreasing temperature and do not show any pronounced unusual effects. The temperature dependences of the longitudinal stiffness and bulk modulus (Fig. 3a and c) can be approximated by the conventional model for vibrational anharmonicity [31]:

$$M = M_0[1 - KF(T/\Theta_D)] \qquad (3)$$

with

$$F(T/\Theta_D) = 3(T/\Theta_D)^4 \int_0^{\Theta_D/T} \frac{x^3\,dx}{e^x - 1}. \qquad (4)$$

Here M refers to elastic moduli, M_0 and K are constants. The shear stiffness and Young's modulus also fit Equation 3, but with a slight deviation below about 175 K (see Fig. 3b and d). The acoustic Debye temperature increases smoothly with decreasing temperature (Fig. 3e) in accord with stiffening of both the longitudinal and shear wave velocities. Poisson's ratio remains practically constant in the whole temperature range of measurements.

4. Hydrostatic-pressure dependences of ultrasonic wave velocity and elastic stiffness moduli

The effects of hydrostatic pressure on ultrasonic wave velocity in AlN ceramic are small (Fig. 4). The longitudinal mode velocity is much more pressure dependent than that of the shear mode. This experimental fact is in line with the results of Gerlich *et al*. [2] but in striking contrast with recent measurements [32] of sound velocity under pressure up to 0.7 GPa, which found surprisingly that shear wave velocity is more pressure dependent than that of the longitudinal wave. The data for the pressure dependence of the velocities of both longitudinal and shear ultrasonic waves are reproducible under pressure cycling and show no measurable hysteresis effects (Fig. 4). This observation indicates that the AlN ceramic does not alter in morphology under pressure cycling up to 0.2 GPa and that there is no relaxation of any residual stress. The velocities of both the longitudinal and shear ultrasonic waves increase approximately linearly with pressure. This is a normal behaviour: both the long-wavelength longitudinal and shear acoustic-modes stiffen under pressure, the effect on the former being much the larger.

The hydrostatic-pressure derivative $(\partial M/\partial P)_{P=0}$ of each elastic stiffness M have been obtained from the

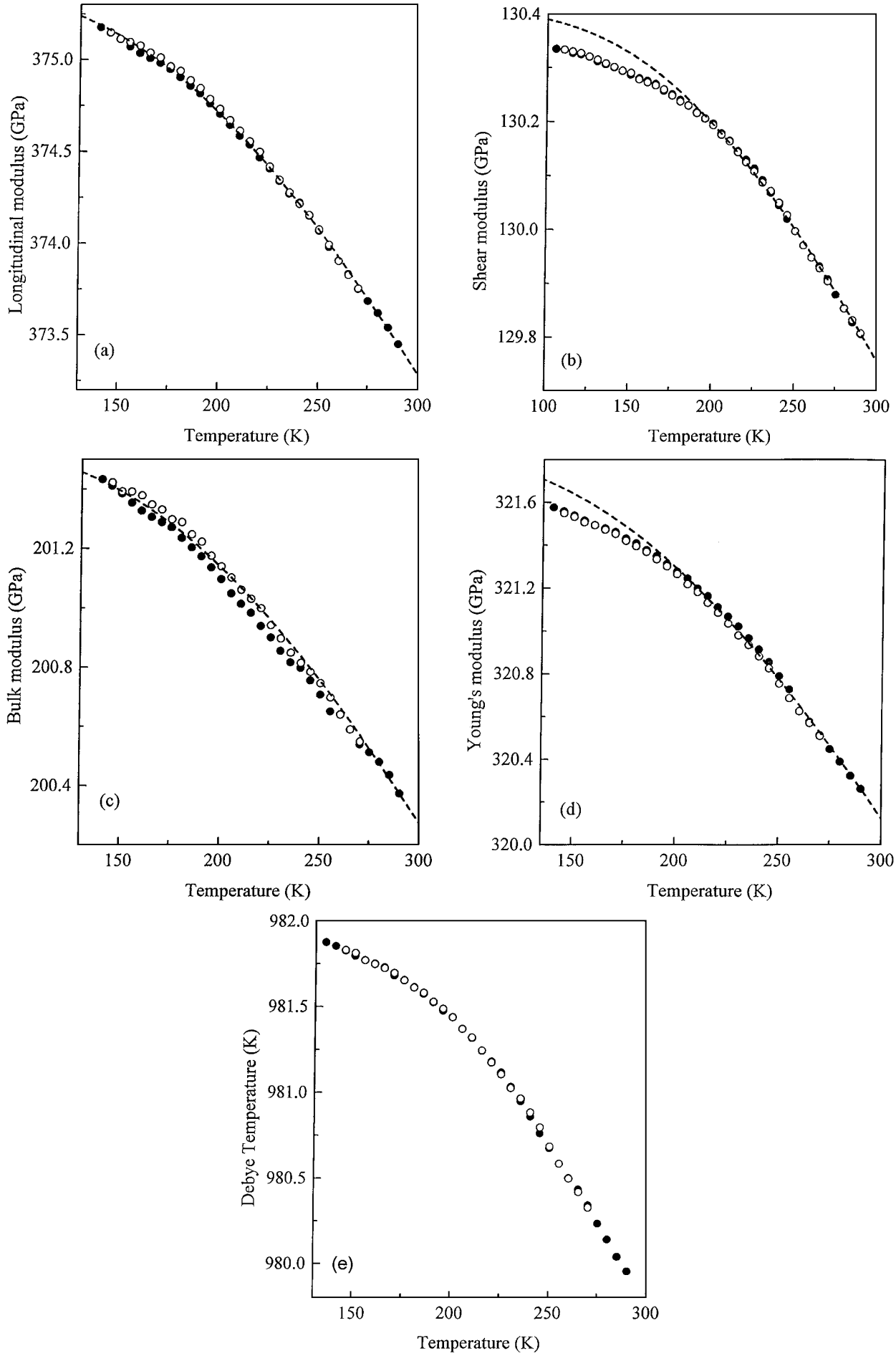

Figure 3 Temperature dependences of the adiabatic elastic moduli of AlN ceramic (a) C_L, (b) μ, (c) B^S, (d) E and (e) acoustic Debye temperature. The filled circles correspond to measurements made with decreasing temperature and the open circles to data obtained as the temperature was increased. The dashed line refers to the calculated elastic moduli using Equation 3.

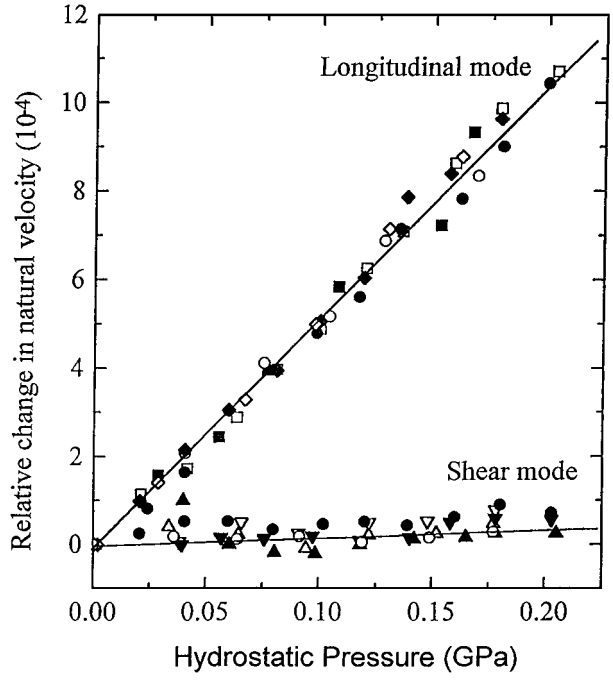

Figure 4 Hydrostatic-pressure dependence of the relative change in natural velocity measured at room temperature. The filled symbols correspond to measurements made with increasing pressure and the open symbols to data as the pressure was decreased (different symbols refer to different experimental runs). The straight lines are for visual guidance.

ultrasonic velocity measurements under pressure by using [33]

$$\left(\frac{\partial M}{\partial P}\right)_{P=0} = (M)_{P=0}\left[\frac{2(\partial f/\partial P)}{f} + \frac{1}{3B^{\mathrm{T}}}\right]_{P=0}, \quad (5)$$

where B^{T} is the isothermal bulk modulus, f is the pulse-echo-overlap frequency at atmospheric pressure and $\partial f/\partial P$ is its pressure derivative. The adiabatic bulk modulus B^{S} has been used rather than B^{T} throughout the calculations, a procedure which introduces only a negligible error. The hydrostatic-pressure derivatives $(\partial C_{\mathrm{L}}/\partial P)_{P=0}$, $(\partial \mu/\partial P)_{P=0}$ and $(\partial B^{\mathrm{S}}/\partial P)_{P=0}$ determined for the AlN ceramic have positive values (Table I) characteristic of a normal solid. Both the longitudinal and shear elastic stiffnesses and thus the slopes of the corresponding acoustic-mode dispersion curves, at the long-wavelength limit, increase with pressure in the normal way. The results obtained for the pressure derivatives of C_{L}, μ and B^{S} are comparable to those determined previously [2] from ultrasonic wave velocity measurements under uniaxial pressure. We note that the experimental errors in the values of pressure derivatives of elastic moduli quoted in [2] are much larger than those in this work, as would be expected because it is possible to apply much greater hydrostatic pressure on a sample without damaging it.

The value determined for the hydrostatic-pressure derivative $(\partial B^{\mathrm{S}}/\partial P)_{P=0}$ of adiabatic bulk modulus of ceramic AlN is compared in Table II with those reported by other researchers using other methods. The value of $(\partial B^{\mathrm{S}}/\partial P)_{P=0}$ is in reasonable agreement with the results of very-high pressure X-ray diffraction measurements [12, 13] and theoretical calculations [18–23] in particular with that derived by Ito [23].

The measurements of the bulk modulus and its hydrostatic-pressure derivative have been used to calculate the volume compression $V(P)/V_0$ of AlN up to high pressures, using an extrapolation method based on the Murnaghan's equation of state [34] in the logarithmic form. The results obtained are in excellent agreement with those of theoretical calculations by Ito [23], which in fact overlap with the present results, Ching and Harmon [18] and Kim *et al*. [22]; the agreement is reasonable with the results of Van Camp *et al*. [19].

5. Grüneisen parameters and acoustic-mode vibrational anharmonicity

The hydrostatic-pressure dependences of ultrasonic wave velocities quantify to first order the vibrational anharmonicity of long-wavelength acoustic modes. Properties of a solid that depend upon thermal motion of the atoms are much influenced by anharmonicity. Common practice is to describe the anharmonic properties in terms of Grüneisen parameters, which quantify the volume or strain dependence of the lattice vibrational frequencies. The dependence of the acoustic-mode frequency ω_{p} in a phonon branch p on volume V can be expressed as a mode Grüneisen parameter

$$\gamma_{\mathrm{p}} = -\left[\frac{\partial(\ln \omega_{\mathrm{p}})}{\partial(\ln V)}\right]_{\mathrm{T}}, \quad (6)$$

which can be obtained from the measurements of the elastic stiffnesses and their pressure derivatives. The longitudinal (γ_{L}) and shear (γ_{S}) acoustic-mode Grüneisen parameters have been determined using

$$\gamma_{\mathrm{L}} = -\frac{1}{6C_{\mathrm{L}}}\left[C_{\mathrm{L}} - 3B^{\mathrm{T}}\left(\frac{\partial C_{\mathrm{L}}}{\partial P}\right)_{P=0}\right] \quad (7)$$

and

$$\gamma_{\mathrm{S}} = -\frac{1}{6\mu}\left[\mu - 3B^{\mathrm{T}}\left(\frac{\partial \mu}{\partial P}\right)_{P=0}\right] \quad (8)$$

respectively. The mean acoustic-mode Grüneisen parameter (γ^{el}), which is a measure of the overall contribution of zone-centre acoustic modes to the lattice vibrational anharmonicity, has been obtained using

$$\gamma^{\mathrm{el}} = \frac{1}{3}(\gamma_{\mathrm{L}} + 2\gamma_{\mathrm{S}}). \quad (9)$$

This expression is strictly valid only at temperatures which are comparable with the acoustic Debye temperature. The results obtained for γ_{L}, γ_{S} and γ^{el} of ceramic AlN at room temperature are included in Table I. All acoustic-mode Grüneisen parameters are positive. The values of γ_{L} and γ^{el} are similar to those determined by Gerlich *et al*. [2], whereas γ_{S} has a small positive value in contrast to the negative value obtained by them. A small value of γ^{el} indicates that the effects of acoustic-mode vibrational anharmonicity are not great. Since AlN has such a high acoustic Debye temperature, the long wavelength acoustic phonons can be expected

to dominate properties determined by vibrational anharmonicity even at room temperature. The thermal Grüneisen parameter γ^{th} ($=3\alpha V B^S/C_P$) has been determined using the linear thermal expansion coefficient (α) [11] and specific heat (C_P) [10] data for AlN. A value of 0.65 has been obtained at room temperature for γ^{th} which is comparable to γ^{el}. Small values for the acoustic-mode Grüneisen parameters and hence low vibrational anharmonicity are compatible with the low thermal expansion of AlN. The mode Grüneisen parameters of the longitudinal optic (LO) and transverse optic (TO) Raman active phonons of AlN were measured [35]: γ_{LO} and γ_{TO} are 1.0 and 1.6, respectively. Recent Raman-scattering studies of aluminum nitride at high pressure [36] yielded the values of 0.38 and 1.58 for γ_{LO} and γ_{TO}, and a value of 1.26 for the Grüneisen parameter of mode $E_2^{(2)}$. First-principles full-potential muffin-tin orbital calculations [22] led to a value of 1.5 for the Grüneisen parameter of the zone-centre TO phonons in AlN. Although the thermal Grüneisen parameter γ^{th} includes the effects of all phonons in the Brillouin zone, contributions from optical phonons are negligible at room temperature. The shear acoustic-mode Grüneisen parameter γ_S ($=0.006$) is much smaller than the longitudinal acoustic-mode Grüneisen parameter γ_L ($=1.09$) accounting for the low thermal Grüneisen parameter γ^{th} ($=0.65$) estimated for this ceramic: since the acoustic Debye temperature Θ_D ($=980 \pm 5$ K) is very high, shear modes play a more important role than longitudinal modes in the acoustic phonon population at room temperature. This enhances their contribution to thermal expansion and specific heat - lowering the thermal expansion and hence the thermal Grüneisen parameter.

6. Conclusions

The velocities of longitudinal and shear 30 MHz ultrasonic waves propagated in hot-pressed AlN ceramic have been measured as functions of temperature and hydrostatic pressure. The AlN ceramic is a comparatively stiff material elastically: its volume-dependent elastic (longitudinal and bulk) moduli and the acoustic Debye temperature are large. Both the longitudinal stiffness and bulk modulus show normal behaviour with temperature and can be fitted to the conventional model for vibrational anharmonicity. The shear stiffness and Young's modulus also fit the model, but with a slight deviation below about 175 K. The hydrostatic-pressure derivatives of the longitudinal and shear elastic stiffnesses and bulk modulus have positive values, hence, the long-wavelength longitudinal, shear and mean acoustic-mode Grüneisen parameters are positive. The thermal properties of AlN are in accord with the low acoustic-mode vibrational anharmonicity.

Acknowledgements

G.A.S. and M.C. are grateful to NATO (Scientific and Environmental Affairs Division, Grant number CRG960584). B.J. is grateful to MOD for Corporate Research Programme funding. We would also like to thank E. F. Lambson, W. A. Lambson and R. C. J. Draper for technical assistance.

References

1. W. M. YIM, E. J. STOFKO, P. J. ZANZUCCHI, J. I. PANKOVE, M. ETTENBERG and S. L. GILBERT, *J. Appl. Phys.* **44** (1973) 292.
2. D. GERLICH, S. L. DOLE and G. A. SLACK, *J. Phys. Chem. Solids* **47** (1986) 437.
3. K. SHIMADA, T. SOTA and K. SUZUKI, *J. Appl. Phys.* **84** (1998) 4951.
4. M. I. MENDELSON, *J. Amer. Ceram. Soc.* **52** (1969) 443.
5. E. P. PAPADAKIS, *J. Acoust. Soc. Am.* **42** (1967) 1045.
6. E. KITTINGER, *Ultrasonics* **15** (1977) 30.
7. R. N. THURSTON and K. BRUGGER, *Phys. Rev.* **133** (1964) A1604.
8. Z. ROSENBERG, N. S. BRAR and S. J. BLESS, *J. Appl. Phys.* **70** (1991) 167.
9. G. SUBHASH and G. RAVICHANDRAN, *J. Mat. Sci.* **33** (1998) 1933.
10. J. C. NIPKO and C.-K. LOONG, *Phys. Rev. B* **57** (1998) 10550.
11. G. A. SLACK and S. F. BARTRAM, *J. Appl. Phys.* **46** (1975) 89.
12. M. UENO, A. ONODERA, O. SHIMOMURA and K. TAKEMURA, *Phys. Rev. B* **45** (1992) 10123.
13. Q. XIA, H. XIA and A. L. RUOFF, *J. Appl. Phys.* **73** (1993) 8198.
14. K. TSUBOUCHI, K. SUGAI and N. MIKOSHIBA, in IEEE Ultrasonics Symposium, (1981) Vol. 1, p. 375.
15. L. E. MCNEIL, M. GRIMSDITCH and R. H. FRENCH, *J. Amer. Ceram. Soc.* **76** (1993) 1132.
16. G. CARLOTTI, F. S. HICKERNELL, H. M. LIAW, L. PALMIERI, G. SOCINO and E. VERONA, in IEEE Ultrasonics Symposium, (1995) Vol. 1, p. 353.
17. C. DEGER, E. BORN, H. ANGERER, O. AMBACHER, M. STUTZMANN, J. HORNSTEINER, E. RIHA and G. FISCHERAUER, *Appl. Phys. Lett.* **72** (1998) 2400.
18. W. Y. CHING and B. N. HARMON, *Phys. Rev. B* **34** (1986) 5305.
19. P. E. VAN CAMP, V. E. VAN DOREN and J. T. DEVREESE, *ibid.* **44** (1991) 9056.
20. Y. N. XU and W. Y. CHING, *ibid.* **48** (1993) 4335.
21. E. RUIZ, S. ALVAREZ and P. ALEMANY, *ibid.* **49** (1994) 7115.
22. K. KIM, W. R. L. LAMBRECHT and B. SEGALL, *ibid.* **53** (1996) 16310.
23. T. ITO, *Jpn. J. Appl. Phys.* **37** (1998) L574.
24. N. E. CHRISTENSEN and I. GORCZYCA, *Phys. Rev. B* **47** (1993) 4307.
25. K. MIWA and A. FUKUMOTO, *ibid.* **48** (1993) 7897.
26. R. KATO and J. HAMA, *J. Phys. Condensed Matter* **6** (1994) 7617.
27. A. F. WRIGHT, *J. Appl. Phys.* **82** (1997) 2833.
28. G. A. SLACK and T. F. MCNELLY, *J. Cryst. Growth* **34** (1976) 263.
29. *Idem., ibid.* **42** (1977) 560.
30. M. UENO, M. YOSHIDA, A. ONODERA, O. SHIMOMURA and K. TAKEMURA, *Phys. Rev. B* **49** (1994) 14.
31. S. C. LAKKAD, *J. Appl. Phys.* **42** (1971) 4277.
32. D. P. DANDEKAR, A. ABBATE and J. FRANKEL, *ibid.* **76** (1994) 4077.
33. R. N. THURSTON, *Proc. IEEE* **53** (1965) 1320.
34. F. D. MURNAGHAN, *Proc. Natl. Acad. Sci. USA* **30** (1944) 244.
35. J. A. SANJURJO, E. LOPEZ-CRUZ, P. VOGL and M. CARDONA, *Phys. Rev. B* **28** (1983) 4579.
36. P. PERLIN, A. POLIAN and T. SUSKI, *ibid.* **47** (1993) 2874.

Received 25 August
and accepted 14 December 1999